Catal Lett (2008) 125:76–82
DOI 10.1007/s10562-008-9513-6

Novel Alumina-Supported PtFe Alloy Nanoparticles for Preferential Oxidation of Carbon Monoxide in Hydrogen

Jie Yin · Junhu Wang · Tao Zhang · Xiaodong Wang

Received: 20 February 2008 / Accepted: 5 May 2008 / Published online: 29 May 2008

Abstract Supported bimetallic PtFe catalyst is one of the most promising candidates for preferential CO oxidation (PROX) in H_2 for fuel cells. We are interested in developing novel PtFe catalysts which have special architectures and are more excellent in catalytic performance for the PROX reaction. In the present study, three kinds of novel alumina-supported PtFe, $PtFe_2$ and $PtFe_3$ alloy nanoparticles were prepared from $Pt(acac)_2$ and $Fe(acac)_3$ reduced by ethylene glycol in Ar atmosphere at 185 °C. The catalytic experiments showed that the three materials were more active for the PROX reaction under pretreatment both in He and H_2 atmospheres as compared to that of Pt/Al_2O_3 prepared by the same chemical route. Their structural property and iron state were investigated by X-ray diffraction and ^{57}Fe Mössbauer spectroscopy. The obtained results proved that the novel as-prepared $PtFe/Al_2O_3$, $PtFe_2/Al_2O_3$ and $PtFe_3/Al_2O_3$ materials are clearly different in the architecture and the oxidation state of iron as compared to the conventionally prepared one.

J. Yin · J. Wang (✉) · T. Zhang (✉) · X. Wang
State Key Laboratory of Catalysis, Dalian Institute of Chemical Physics, Chinese Academy of Sciences, 457 Zhongshan Road, Dalian 116023, China
e-mail: wangjh@dicp.ac.cn

T. Zhang
e-mail: taozhang@dicp.ac.cn

J. Yin
Graduate School of Chinese Academy of Sciences, Beijing 100039, China

Keywords PtFe bimetallic catalyst · Alloy nanoparticle · Iron oxidation state · Structural property · Catalytic mechanism · PROX reaction

1 Introduction

There is wide interest in the development of novel heterogeneous catalysts that are applicable to the carbon monoxide (CO) preferential oxidation (PROX) in rich-hydrogen atmosphere to improve the efficiency of fuel cells [1–10]. Development of the novel heterogeneous catalysts as cathode for polymer electrolyte membrane (PEM) fuel cells is also in the field of vision [11, 12]. Among the reported heterogeneous catalysts so far for the CO oxidation, PROX reaction and cathodic materials of the PEM fuel cells, supported Pt-Fe nanoparticles prepared by one improved method have been investigated by several groups [3–6, 8]. Liu et al. reported an iron oxide promoted Pt/Al_2O_3 catalyst prepared by a modified impregnation method and investigated the role of iron in enhancing the catalytic performance for the PROX reaction [3]. Kotobuki et al. reported the catalytic mechanism of the PROX reaction on Pt, Fe and Pt-Fe/mordentite catalysts prepared by a conventional ion-exchange method [4]. They proposed a so-called "bifunctional mechanism" and pointed out that the mechanism was clearly different to that of the PROX reaction on Au catalysts supported on TiO_2, Al_2O_3 and ZrO_2 [7]. They also confirmed that Pt forms the metallic clusters after H_2 pretreatment or the PROX reaction, whereas a large part of Fe exists as oxides even after the H_2 treatment according to a XAFS characterization [5]. Tang et al. reported novel $Pt\text{-}Fe/Al_2O_3$ catalyst prepared by a modified polylol method, which showed 99% CO conversion and 98% selectivity at 80 °C and $n(CO)/n(O_2) = 2$ [6].

Very recently, Siani et al. reported the silica-supported Pt, $PtFe_2$ and Pt_5Fe_2 catalysts prepared from $PtFe_2(COD)(CO)_8$ (COD = 1,5-cyclooctadiene) and $Pt_5Fe_2(COD)_2(CO)_{12}$ organometallic cluster precursors, respectively [8]. They gained better control on the stoichiometry and morphology of the resulting Pt-Fe nanoparticles due to use the above two bimetallic Pt-Fe clusters as precursor. The cluster-derived $PtFe/SiO_2$ catalyst showed improved CO oxidation activity in the presence and absence of hydrogen as compared to that prepared by the conventional methods. However, we still have a doubt whether the best composition of the supported bimetallic Pt-Fe catalyst was found or not due to the limited composition of the cluster precursor. On the other hand, the chemical synthesis of self-assembled and monodispersed PtFe alloy nanoparticles have been widely investigated for the new generation ultra density magnetic storage [13–20].

It is interesting to develop novel supported chemically disordered and/or ordered PtFe alloy nanoparticles and deeply investigate their catalytic mechanism of the PROX reaction by mainly using ^{57}Fe Mössbauer Mössbauer spectroscopy under various experimental conditions. In the present study, the results of three kinds of novel alumina-supported $PtFe_x$ (x = 1, 2 and 3) alloy nanoparticles, which were prepared by modifying the reported chemical process [13–20], are described for the enhanced activity and selectivity at low temperatures (< 100 °C) for the PROX reaction and for the structural characterization by using ^{57}Fe Mössbauer Mössbauer spectroscopy and X-ray diffraction (XRD).

2 Experimental

2.1 Material Preparation

The samples used in this study were described in Table 1. One kind of PtFe alloy nanoparticles and three kinds of alumina-supported PtFe, $PtFe_2$ and $PtFe_3$ alloy nanoparticles were synthesized. Synthesis experiment of PtFe alloy nanoparticles were carried out using $Pt(acac)_2$ (acac = acetylacetonato) and $Fe(acac)_3$ purchased from Alfa company without any further purification. In short, first, the desired amounts of Pt and Fe precursors were dissolved in 100 cm^3 of ethylene glycol (analytic reagent) in a vessel with reflux attachment; second, the vessel was placed in an oil bath and the air gas in the vessel was replaced by Ar gas; third, the mixed solution was mechanically stirred and heated at a constant rate under Ar gas flowing and then kept at 185 °C for 3 h. After cooling, the PtFe nanoparticles were centrifugally separated, washed by ethanol, dried at 60 °C in vacuum over one night and then used to XRD and Mössbauer Mössbauer characterizations.

Table 1 Compositions of the samples used in this study

Weight percent	Pt/Fe mole ratio
PtFe nanoparticles	PtFe
$3\%Pt/Al_2O_3$	–
$2.58\%Fe/Al_2O_3$	–
$3\%Pt\text{-}0.86\%Fe/Al_2O_3$	$PtFe/Al_2O_3$
$3\%Pt\text{-}1.72\%Fe/Al_2O_3$	$PtFe_2/Al_2O_3$
$3\%Pt\text{-}2.58\%Fe/Al_2O_3$	$PtFe_3/Al_2O_3$

Procedures for synthesizing the alumina-supported $PtFe_x$ alloy nanoparticles were the same as that of the PtFe alloy nanoparticles till the step keeping at 185 °C for 3 3 h. After reducing the temperature to 100 °C, desired amounts of the γ-Al_2O_3 support with a BET area of 227 227 m^2 m^2 g^{-1} were added to the solution and continued to mechanically stirred for 12 12 h under Ar flowing. The alumina-supported PtFe, $PtFe_2$ and $PtFe_3$ alloy nanoparticles were filtered by sucking, washed by ethanol, dried at 60 °C in vacuum over one night and then used to the PROX reaction, XRD and Mössbauer Mössbauer characterization. For a comparison, Pt/Al_2O_3 and Fe/Al_2O_3 were also synthesized by the same process by only using the Pt or Fe precursors.

2.2 XRD and ^{57}Fe Mössbauer Characterizations

A conventional ANA analytical X'pert Pro Super model diffractometer with Cu Kα radiation (λ = 1.5432 Å) was used at room temperature for examining whether the as-prepared PtFe nanoparticles are alloy or not. The ^{57}Fe Mössbauer spectra of the as-prepared materials were recorded using a Topologic 500A spectrometer and a proportional counter at room temperature. ^{57}Co(Rh) moving in a constant acceleration mode was used as radioactive source. ^{57}Fe Mössbauer spectral parameters such as the isomer shift (IS), the electric quadrupole splitting (QS) and the relative spectral areas of the different components of the absorption patterns were evaluated.

2.3 Evaluation of Catalytic Performance

The catalytic performances to the PROX reaction over the alumina-supported Pt, PtFe, $PtFe_2$ and $PtFe_3$ alloy nanoparticles were measured in a fixed-bed reactor at atmospheric pressure using 100 mg of the catalysts heated at He and H_2 atmospheres, respectively [9, 10]. The reaction gas ($2\%CO+40\%H_2+1\%O_2$ balanced by He) passed through the catalyst bed with a space velocity of 40,000 cm^3 g^{-1} h^{-1}. The inlet and outlet gas composition was analyzed by an on-line gas chromatograph (Angilent GC-8800) with a TCD (thermal conductivity) detector. Before the catalytic performance measurement, the catalyst

powder was pelletized and then sieved to obtain 40–60 mesh fractions. Quartz particles (120 mg) were added to each of them to maintain the catalyst bed isothermal. Moreover, the samples were separately pre-treated by heating in a He and H_2 flowing atmospheres for 1 h at 400 °C before the PROX reaction. The CO conversion, O_2 conversion and CO_2 selectivity were calculated as follows:

$$\text{CO conversion } (\%) = [\text{CO}]_{\text{in}} - [\text{CO}]_{out} / [\text{CO}]_{in} \times 100\%$$

$$\text{O}_2 \text{ conversion}(\%) = [\text{O}_2]_{in} - [\text{O}_2]_{out} / [\text{O}_2]_{in} \times 100\%$$

$$\text{CO}_2 \text{ selectivity}(\%) = \text{CO conversion } (\%)/\text{O}_2 \text{ conversion } (\%) \times 100\%$$

Where $[CO]_{in}$ and $[CO]_{out}$ are the concentration of CO at the inlet and outlet, respectively. $[O_2]_{in}$ and $[O_2]_{out}$ are the concentration of oxygen at the inlet and outlet, respectively.

3 Results and Discussion

3.1 Catalytic Performance

The effect of alumina-supported Fe alloyed with Pt catalysts can be readily seen by comparing the CO conversion of the PROX reaction over monometallic Pt and bimetallic $PtFe_x$ alloy nanoparticles supported on γ-Al_2O_3, as shown in Fig. 1a. Under our experimental conditions, the B sample exhibited to be hardly active for the PROX reaction at 40–120 °C. However, dramatic improvements were observed in the CO conversion for the alumina-supported PtFe, $PtFe_2$ and $PtFe_3$ alloy nanoparticles at 40–120 °C after the addition of iron. The CO conversion increased initially with the reaction temperature and had a maximum of 41% at 120 °C, 49% and 33% at 100 °C for the alumina-supported PtFe, $PtFe_2$ and $PtFe_3$ alloy nanoparticles, respectively. The alumina-supported $PtFe_2$ alloy nanoparticles showed the highest CO conversion at 40–100 °C among the three alumina-supported bimetallic $PtFe_x$ samples. In addition, a relative steady-state CO conversion was observed at 80–120 °C over the alumina-supported PtFe and $PtFe_2$ alloy nanoparticles, which was higher than that of the alumina-supported $PtFe_3$ alloy nanoparticles above 100 °C. Though the CO conversions for the three alumina-supported bimetallic $PtFe_x$ samples were not higher than that of Pt-Fe/Al_2O_3 [5], Pt-Fe/mordenite [4] and cluster-derived PtFe/SiO_2 [7] catalysts, the promoting effect to the PROX reaction was clearly confirmed due to the addition of iron to Pt/Al_2O_3 in the present study.

Another indicator that the three alumina-supported bimetallic $PtFe_x$ samples promoted the PROX reaction was reflected in their high selectivity for CO_2 at low temperature. As shown in Fig. 1b, comparing with that of the alumina-supported Pt catalyst, the CO_2 selectivity was clearly improved at 40–80 °C. The CO_2 selectivity reached to 90%, 59% and 74% for the alumina-supported PtFe, $PtFe_2$ and $PtFe_3$ alloy nanoparticles at 40 °C, respectively. Though the alumina-supported $PtFe_2$ alloy nanoparticles showed the highest CO conversion, its CO_2 selectivity was the lowest among the three alumina-supported bimetallic $PtFe_x$ samples at 40–80 °C. It indicated that the relative amounts of Pt and Fe (Pt/Fe atomic ratios) also influenced the CO_2 selectivity.

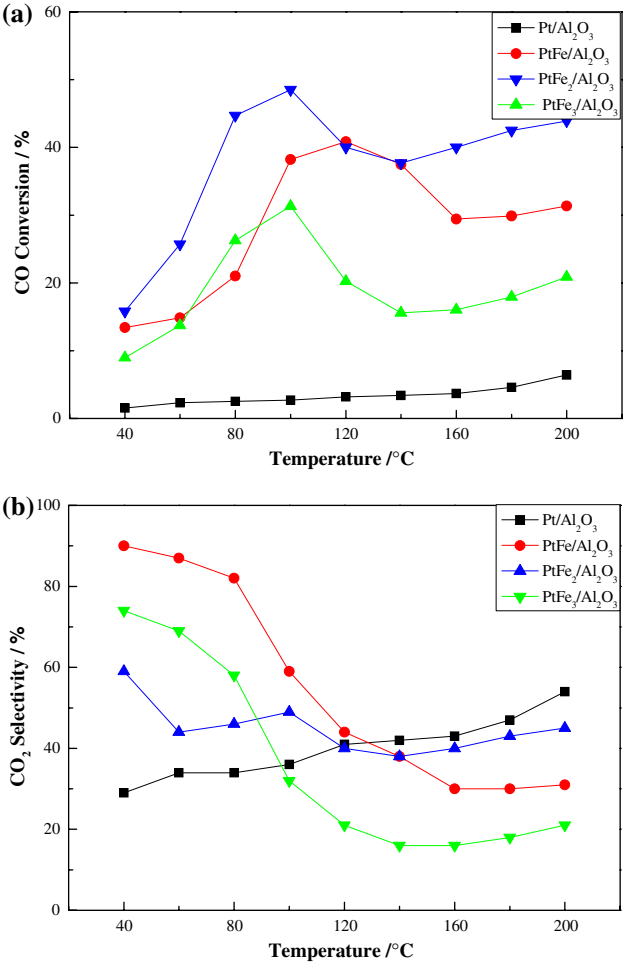

Fig. 1 CO conversion (a) and CO_2 selectivity (b) against reaction temperature during the PROX reaction on Pt/Al_2O_3, PtFe/Al_2O_3, $PtFe_2$/Al_2O_3 and $PtFe_3$/Al_2O_3 pretreated in H_2 at 400 °C for 2 h. (Catalyst: 100 mg mixed with 120 mg quartz particles; reaction gas: 2%CO+40%H_2+1%O_2 balanced by He; space velocity: 40,000 $cm^3\ g^{-1}\ h^{-1}$)

3.2 XRD Characterization

The XRD results, as shown in Fig. 2, indicated that the PtFe nanoparticles are pure chemically disordered face central cubic (fcc) structure (Fig. 2a) with a lattice constant of 3.849 Å and annealing at 600 °C under N_2 atmosphere

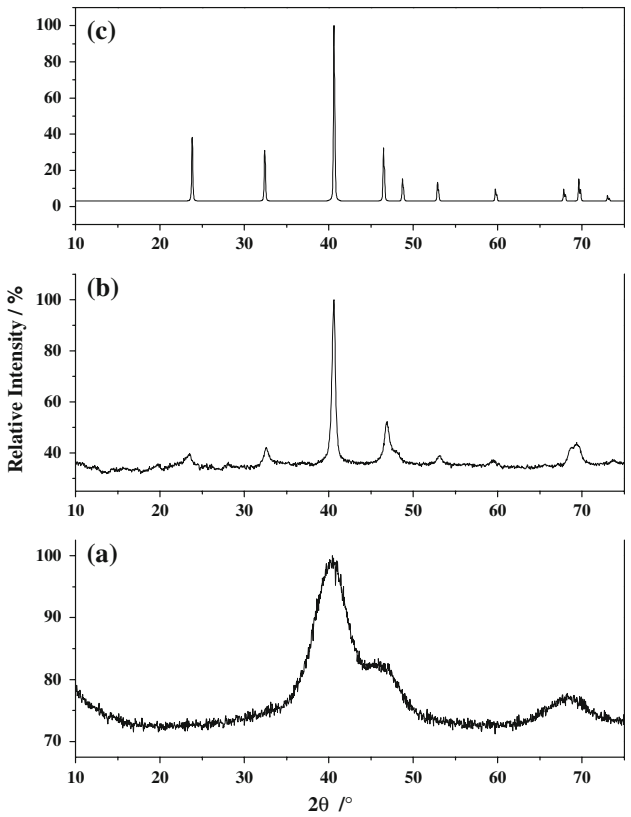

Fig. 2 X-ray diffraction patterns of the as-prepared PtFe alloy nanoparticles before (a) and after (b) heat treatment also including the standard patterns of the ordered fct PtFe alloy

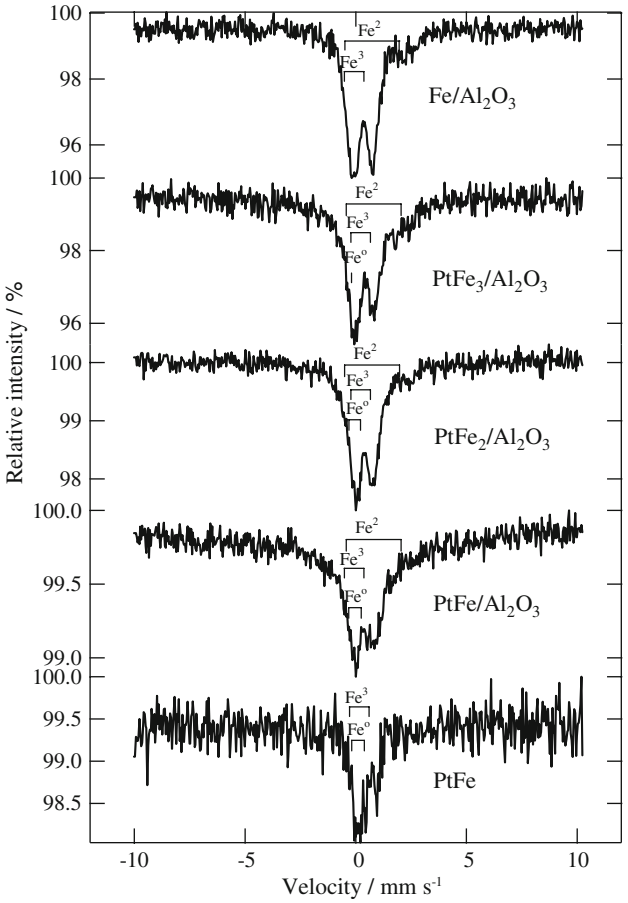

Fig. 3 ^{57}Fe Mössbauer spectra of the as-prepared alumina-supported $PtFe_x$ alloy nanoparticles at room temperature also including that of the as-prepared fcc disordered PtFe alloy nanoparticles and Fe/Al_2O_3

induces the Pt and Fe atoms to rearrange into the long-range chemically ordered face central tetragonal (fct) structure as shown in Fig. 2b. It was consistent with that reported so far [13–19] and clearly revealed that Fe alloyed with Pt in the as-prepared PtFe nanoparticles. Figure. 2c shows the standard patterns of the fct PtFe alloy. The broad peaks shown in Fig. 2a originated from small diameter of the as-prepared PtFe alloy nanoparticles, which its particle size was estimated with Scherrer's formula to be 2.1 nm. By the way, the crystal structure of the A sample was stable as confirmed by comparing the XRD patterns before and after keeping the PtFe nanoparticles in air for one month.

3.3 ^{57}Fe Mössbauer Characterization

Mössbauer technique is effective to the identification of catalyst components in terms of active phase or active sites and search for correlations between these components and one or more of the catalytic properties [21–28]. Here, ^{57}Fe Mössbauer spectroscopy was employed to characterize the iron state in the as-prepared materials. Figure. 3 shows the ^{57}Fe Mössbauer spectra of the as-prepared alumina-supported $PtFe_x$ alloy nanoparticles at room temperature. For a comparison, the PtFe nanoparticles and Fe/Al_2O_3 were also characterized by ^{57}Fe Mössbauer spectroscopy. The spectrum of the PtFe nanoparticles was similar to that of the alumina-supported PtFe, $PtFe_2$ and $PtFe_3$ alloy nanoparticles, which mainly consist of one alloyed iron and one ferric quadrupole doublet. The spectrum of the Fe/Al_2O_3 sample exhibited a different pattern, which consist of one ferric and one ferrous quadrupole doublet. Small amounts of ferrous component were also observed in the spectra of the alumina-supported PtFe, $PtFe_2$ and $PtFe_3$ alloy nanoparticles. The ferrous component was possible to be produced by the addition of acidic alumina support since it was not observed in the spectrum of the Fe/Al_2O_3 sample.

Taking into consideration on a very recent report that small monodispersed FeO nanoparticles were synthesized through reductive decomposition of $Fe(acac)_3$ with oleic acid and oleylamine both as surfactants and solvents at 220–300 °C [29], we can speculate that partial ferric irons were only reduced and stabilized in ferrous state due to the addition of γ-Al_2O_3 even in the existence of a noble metal promoter like Pt in the chemical process used in the present study. This is reasonable since the ethylene glycol and

Table 2 ^{57}Fe Mössbauer parameters of PtFe alloy nanoparticles and novel alumina-supported $PtFe_x$ alloy nanoparticles at room temperature

Composition	Oxidation state of iron	IS[a] (mm s^{-1})	QS[b] (mm s^{-1})	Spectral area (%)[c]
PtFe	Fe^{3+}	0.32	0.96	50
	Alloy	0.35	0.34	50
Fe/Al_2O_3	Fe^{3+}	0.32	0.88	82
	Fe^{2+}	1.17	2.06	18
$PtFe/Al_2O_3$	Fe^{3+}	0.30	0.91	50
	Fe^{2+}	1.15	1.99	3
	Alloy	0.35	0.35	47
$PtFe_2/Al_2O_3$	Fe^{3+}	0.33	0.87	75
	Fe^{2+}	1.16	2.02	10
	Alloy	0.33	0.32	15
$PtFe_3/Al_2O_3$	Fe^{3+}	0.32	1.04	60
	Fe^{2+}	1.05	1.95	15
	Alloy	0.18	0	25

[a] IS, isomer shift; [b] QS, electric quadrupole splitting; [c] Uncertainty is ±5% of reported value

oleic acid or oleylamine are relatively soft reducer. The results also implied that a strongly chemical interaction existed between the support of γ-Al_2O_3 and the PtFe alloy nanoparticles.

Table 2 lists the evaluated ^{57}Fe Mössbauer parameters. The relative resonance area of the ferrous species decreased in the increase of Pt molar fractions contained in the as-prepared catalysts, i.e. Fe^{2+} in $PtFe/Al_2O_3 < PtFe_2/Al_2O_3 < PtFe_3/Al_2O_3 < Fe/Al_2O_3$, Pt molar fraction in $PtFe/Al_2O_3 > PtFe_2/Al_2O_3 > PtFe_3/Al_2O_3 > Fe/Al_2O_3$. It is known that noble metal like Pt can enhance the reduction of iron intimately contacting with them in the supported bimetallic catalysts [21]. The phenomenon was confirmed here by the ^{57}Fe Mössbauer technique. The IS and QS values of the alloyed iron were evaluated to be 0.35 and 0.35 mm s^{-1} for the $PtFe/Al_2O_3$ sample, 0.33 and 0.32 mm s^{-1} for the $PtFe_2/Al_2O_3$ sample and 0.18 and 0 mm s^{-1} for the $PtFe_3/Al_2O_3$ sample. It means that the s-density at the iron nuclear position in the $PtFe/Al_2O_3$ and $PtFe_2/Al_2O_3$ samples is smaller than that of the $PtFe_3/Al_2O_3$ sample, however, the symmetry of the charge distribution at the iron nuclear position in the $PtFe_3/Al_2O_3$ sample is higher than that of the $PtFe/Al_2O_3$ and $PtFe_2/Al_2O_3$ samples [28]. These ^{57}Fe Mössbauer results clearly indicated that the PtFe, $PtFe_2$ and $PtFe_3$ nanoparticles supported on the alumina were still maintained in the alloyed state.

Comparing with the Mössbauer results of the catalysts with the same or similar composition prepared by the conventional method, the ^{57}Fe spectrum shapes of the Fe/Al_2O_3, $PtFe/Al_2O_3$, $PtFe_2/Al_2O_3$ and $PtFe_3/Al_2O_3$ samples are more similar to that reduced in H_2 atmosphere above 400 °C [21, 23, 24, 26]. As reported so far, all of the alumina-supported Fe and Pt-Fe catalysts prepared initially by the conventional method contained iron only in the ferric state, the metallic iron and/or ferrous components appeared after the H_2 or CO reduction, as determined by ^{57}Fe Mössbauer spectroscopy [21]. XAFS characterization of the as-prepared Pt-Fe/zeolite catalyst, which was noted as "ion-exchanged" catalyst by Kotobuki et al., also showed that Fe existed only as Fe^{3+} before the H_2 pre-treatment and the PROX reaction [5]. However, the as-prepared alumina-supported $PtFe_x$ alloy nanoparticles in the present study contained iron not only in the ferric state but also in the alloyed iron and ferrous states. Furthermore, the oxidation states of iron in the as-prepared samples were stable, which was also confirmed by the Mössbauer results of the PtFe nanoparticles keeping in air before and after one month.

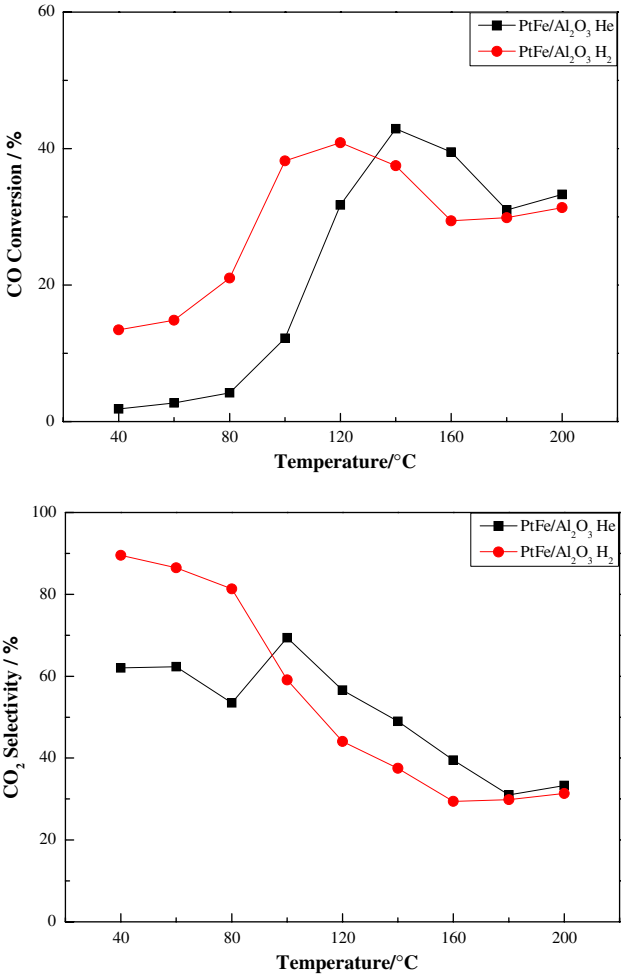

Fig. 4 CO conversion (a) and CO_2 selectivity (b) against reaction temperature during the PROX reaction on $PtFe/Al_2O_3$ separately heated in He and H_2 at 400 °C for 2 h. (Catalyst: 100 mg mixed with 120 mg quartz particles; reaction gas: 2%CO+40%H_2+1%O_2 balanced by He; space velocity: 40,000 cm^3 g^{-1} h^{-1})

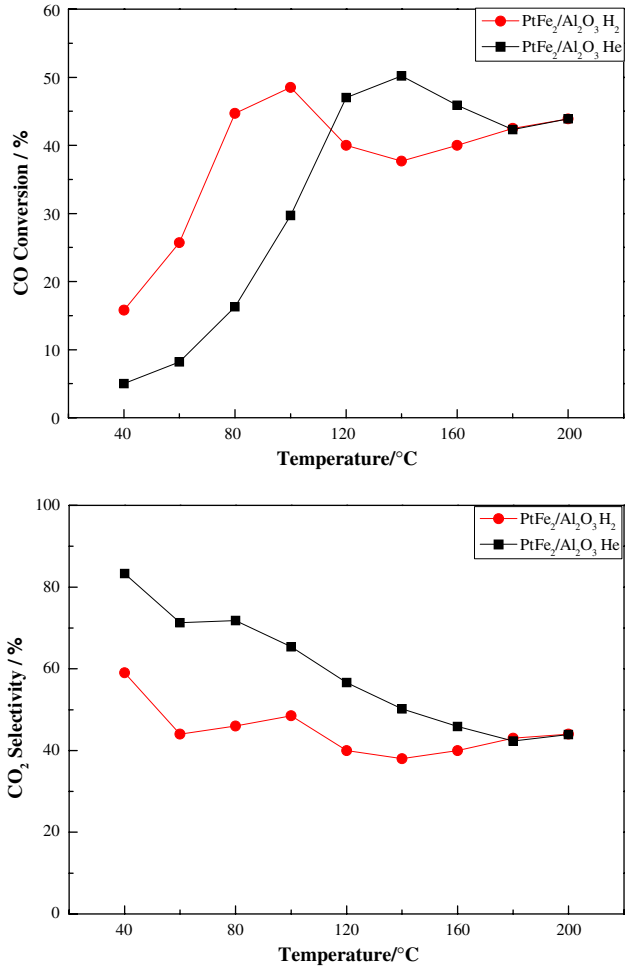

Fig. 5 CO conversion (a) and CO_2 selectivity (b) against reaction temperature during the PROX reaction on $PtFe_2/Al_2O_3$ separately heated in He and H_2 at 400 °C for 2 h. (Catalyst: 100 mg mixed with 120 mg quartz particles; reaction gas: 2%CO+40%H_2+1%O_2 balanced by He; space velocity: 40,000 $cm^3\ g^{-1}\ h^{-1}$)

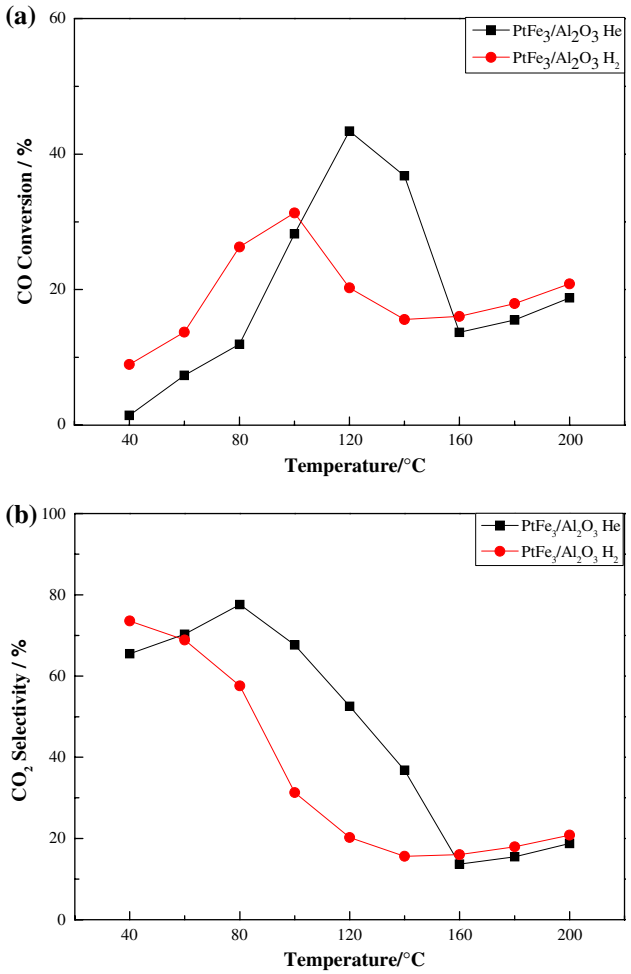

Fig. 6 CO conversion (a) and CO_2 selectivity (b) against reaction temperature during the PROX reaction on $PtFe_3/Al_2O_3$ separately heated in He and H_2 at 400 °C for 2 h. (Catalyst: 100 mg mixed with 120 mg quartz particles; reaction gas: 2%CO+40%H_2+1%O_2 balanced by He; space velocity: 40,000 $cm^3\ g^{-1}\ h^{-1}$)

The catalytic performance over the $PtFe/Al_2O_3$, $PtFe_2/Al_2O_3$ and $PtFe_3/Al_2O_3$ samples were also investigated without the H_2 reduction. The results indicated that at the low temperature range, there was no large difference in the activity and product selectivity within the experimental error over the $PtFe/Al_2O_3$, $PtFe_2/Al_2O_3$ and $PtFe_3/Al_2O_3$ samples as shown in Figs. 4, 5, 6. It implied that the $PtFe/Al_2O_3$, $PtFe_2/Al_2O_3$ and $PtFe_3/Al_2O_3$ samples are not regularly reduced at one high temperature before the PROX reaction. That is to say, they are essentially active to the PROX reaction before the pretreatment of the H_2 reduction or we can say that they are readily activated as compared to the conventionally prepared one. It was known that the H_2 pretreatment of the iron-containing catalysts is for reducing the surface ferric species into ferrous and/or metallic iron species and then activating them.

Taking into consideration of the results obtained from XRD and Mössbauer Mössbauer characterization and the catalytic performance, we can conclude here that the three alumina-supported $PtFe_x$ alloyed catalysts are clearly different in the architectures and the oxidation state of iron as compared with that reported so far. These differences are available to change somewhat the catalytic mechanism in the PROX reaction over the alumina-supported Pt-Fe bimetallic catalyst. Further, the as-prepared $PtFe/Al_2O_3$, $PtFe_2/Al_2O_3$ and $PtFe_3/Al_2O_3$ samples are active to the PROX reaction even without the reduction pretreatment.

Up to know, a noncompetitive dual site mechanism has been proposed for the PROX reaction over the supported bimetallic Pt-Fe catalyst [4–6, 8]. It means that platinum site in Pt^o state acts as CO adsorption site and iron site in FeO_x or Fe^o state as an O_2 dissociative-adsorption site enhances the surface reaction between the reactants on the neighboring sites. The catalytic performance was found to be more active due to the cluster formation between Pt and Fe as compared to the conventionally prepared one [8]. The

reason was concluded not only due to the higher degree of metal dispersion and homogenous mixing of the metals but also due to the direct bonding between Pt atoms and Fe^{n+} ions or reduced Fe^{o} atoms. Here, the noncompetitive dual site mechanism was also considered to be suited to the three alumina-supported $PtFe_x$ alloyed catalysts. The prepared catalysts in the present study should have a narrower size distribution (between 1.5 and -3.5 nm confirmed by HRTEM) and more homogeneous composition due to the employment of the special chemical process and the organic salt as the precursors. The Pt atoms should be more intimately contacted with that the Fe atoms since the Pt atoms alloyed with Fe. These should be benefit to improve the catalytic performance in the PROX reaction over the bimetallic Pt-Fe catalyst.

4 Conclusion

In conclusion, $PtFe/Al_2O_3$, $PtFe_2/Al_2O_3$ and $PtFe_3/Al_2O_3$ materials prepared from $Pt(acac)_2$, $Fe(acac)_3$ and ethylene glycol as a soft reducer in Ar at 185 °C were confirmed to be more active for the PROX reaction as compared to that of Pt/Al_2O_3 material prepared by the same chemical route. The XRD and ^{57}Fe Mössbauer results indicate that PtFe, $PtFe_2$ and $PtFe_3$ nanoparticles supported on alumina are in high dispersion and exist as alloyed state. The oxidation states of iron contained in them are not only in the alloyed Fe^{o} state but also in the ferric and ferrous states as determined by ^{57}Fe Mössbauer spectroscopy. Comparing with that of the PtFe alloy nanoparticles, the ferrous component appeared in ^{57}Fe Mössbauer spectra of the alumina-supported Fe, PtFe, $PtFe_2$ and $PtFe_3$ alloy nanoparticles, which implies that the strongly chemical interaction exists between the nanoparticles and the γ-Al_2O_3 support. The relative resonance area of the ferrous species decreased in the increase of Pt molar fractions contained in the as-prepared catalysts, indicating that Pt can enhance the reduction of iron intimately contacting with them. There were no large difference in the activity and product selectivity within the experimental error over $PtFe/Al_2O_3$, $PtFe_2/Al_2O_3$ and $PtFe_3/Al_2O_3$ treated in H_2 as compared to that treated in He at 400 °C. These results clearly proved that the novel as-prepared $PtFe/Al_2O_3$, $PtFe_2/Al_2O_3$ and $PtFe_3/Al_2O_3$ materials are different in the architecture and the oxidation state of iron as compared to the conventionally prepared one. These differences are reasonable to lead their catalytic performance and mechanism changed somewhat. The present study is essentially benefit to obtaining a completed exploration on the catalytic mechanism of the PROX reaction over the bimetallic Pt-Fe catalyst.

Acknowledgments Financial supports from Dalian Institute of Chemical Physics, Chinese Academy of Sciences for DICP "100 Talents" (No. K703181B01) to J. Wang and from the National Science Foundation of China for Distinguished Young Scientists (No.20325620) to T. Zhang are gratefully acknowledged.

References

1. Korotkikh O, Farrauto R (2000) Catal Today 62:249
2. Son IH, Lane AM (2001) Catal Lett 76:151
3. Liu X, Korotkikh O, Farrauto R (2002) Appl Catal A: Gen 226:293
4. Kotobuki M, Watanabe A, Uchida H, Yamashita H, Watanabe M (2005) J Catal 236:262
5. Kotobuki M, Shido T, Tada M, Uchida H, Yamashita H, Iwasawa Y, Watanabe M (2003) Catal Lett 103:263
6. Tang X, Zhang B, Li Y, Xin Q, Shen W (2005) Chin J Catal 26:1
7. Daniells ST, Overweg AR, Makkee M, Moulijn JA (2005) J Catal 230:52
8. Siani A, Captain B, Alexeev OS, Stafyla E, Hungria AB, Midgley PA, Thomas JM, Adams RD, Amiridis MD (2006) Langmuir 22:5160
9. Huang Y, Wang A, Wang X, Zhang T (2007) Int J Hydrogen Energy 32:3880
10. Zhang W, Wang A, Li L, Wang X, Zhang T (2008) Catal Taday 131:457
11. Igarashi H, Fujino T, Zhu Y, Uchida H, Watanabe M (2001) Phys Chem Chem Phys 3:306
12. Santiago EI, Varanda LC, Villullas HM (2007) J Phys Chem C 111:3146
13. Sun S, Murray CB, Weller D, Folks L, Moser A (2000) Science 287:1989
14. Jeyadevan B, Hobo A, Urakawa K, Chinnasamy CN, Shinoda K, Tohji K (2003) J Appl Phys 93:7574
15. Jeyadevan B, Urakawa K, Hobo A, Chinnasamy N, Shinoda K, Tohji K, Djayaprawira DDJ, Tsunoda M, Takahashi M (2003) Jpn J Appl Phys 42:L350
16. Stahl B, Ellrich J, Thessmann R, Ghafari M, Bahattacharya S, Hahn H, Gajbhiye NS, Kramer D, Viswanath RN, Weissmuller J, Gleiter H (2003) Phys Rev B 67:14422
17. Liu C, Wu X, Klemmer T, Shukla N, Yang X, Weller D, Roy AG, Tanase M, Laughlin D (2004) J Phys Chem B 108:6121
18. Saita S, Maenosono S (2005) Chem Mater 17:3705
19. Rutledge RD, Morris WH, Wellons MS, Gai Z, Shen J, Bentley J, Wittig JE, Lukehart CM (2006) J Am Chem Soc 128:14210
20. Wang C, Hou Y, Kim J, Sun S (2007) Angew Chem Int Ed 46:6333
21. Vannice MA, Garten RL (1975/1976) J Mol Catal 1: 201
22. Berry FJ (1984) Mössbauer spectroscopy applied to inorganic chemistry, vol 1. Plenum Press, New York, p 391
23. Niemantsverdriet JW, Van Kaam JAC, Flipse CFJ, Van Der Kraan AM (1985) J Catal 96:58
24. Fukuoka A, Kimura T, Kosugi N, Kuroda H, Minai Y, Sakai Y, Tominaga T, Ichikawa M (1990) J Catal 126:434
25. Lin L, Yang W, Jia J, Xu Z, Zhang T, Fan Y, Kou Y, Shen J (1999) Sci China B 42:571
26. Stievano L (2000) Hyperfine Interact 126:101
27. Wang J, Ozawa K, Takahashi M, Takeda M, Nonami T (2006) Chem Mater 18:2261
28. Millet JMM (2007) Adv Catal 51:309
29. Hou Y, Xu Z, Sun S (2007) Angew Chem Int Ed 46:6329